

Spatial varying profiling of air PM constituents using paper-based microfluidics

Cite as: Biomicrofluidics 13, 054103 (2019); doi: 10.1063/1.5119910

Submitted: 14 July 2019 · Accepted: 1 September 2019 ·

Published Online: 17 September 2019



View Online



Export Citation



CrossMark

Yuan Jia,^{1,2} Wenyu Wu,¹ Jianping Zheng,³ Zhonghua Ni,^{1,2,a)} and Hao Sun^{4,5,a)}

AFFILIATIONS

¹School of Mechanical Engineering, Southeast University, Nanjing 210096, China

²Jiangsu Key Laboratory for Design and Manufacture of Micro-Nano Biomedical Instruments, Southeast University, Nanjing 211189, China

³Department of Medical Oncology, Fujian Provincial Hospital, Fujian 350001, China

⁴School of Mechanical Engineering and Automation, Fuzhou University, Fuzhou 350116, China

⁵Fujian Provincial Collaborative Innovation Center of High-End Equipment Manufacturing, Fuzhou 350001, China

a)Authors to whom correspondence should be addressed: nzh2003@seu.edu.cn. Tel.: +86 02552090504 and sh@fzu.edu.cn.

Tel.: +86 059122866794.

ABSTRACT

Accurate and quantitative profiling of air particulate matter (PM) compositions is essential for assessing local pollution information. The method combining mobile aerial sampling using unmanned aerial vehicles (UAVs) and prompt analysis excels in this regard as it allows spatiotemporal mapping of air pollution, especially in the vertical direction. However, applications of the method are still scarce as it is limited by a lack of sampling reliability due to insufficient aerial sampling time and a lack of accurate, portable quantification techniques. In this work, by integrating mobile aerial sampling with in-flight tethered charging and smartphone-based colorimetric analysis in a cost-effective paper microfluidic device, we present a method for quantitative, reliable profiling of spatiotemporal variation in air PM compositions. The method extends aerial sampling time to 12–15 flight hours per deployment, thereby significantly improving sampling reliability while maintaining the maneuverability of the UAVs. Also, smartphone-based colorimetric analysis combined with paper-based microfluidics enables portable, economically efficient analysis and is well-suited for using in low-resource settings. We demonstrated the utility of the method by carrying out a spatiotemporal variation study of air PM trace metal components (Fe, Ni, and Mn) at 4 geographical locations in Fuzhou, China, for a period of 21 days, and the results were in good agreement with results obtained from using a commercial instrument. Beside air PM composition study, this method is universally applicable and holds great potential to be extended to multipollutant analysis, such as prompt detection of airborne viruses, bacteria, and others.

Published under license by AIP Publishing. <https://doi.org/10.1063/1.5119910>

INTRODUCTION

Knowledge of air particulate matter (PM) compositions is essential for assessing local air conditions.^{1–3} In addition, air PM constituents such as nitrates, sulfates, organic compounds, biological compounds, and airborne trace metals at elevated concentrations are known as systemic toxicants to human health, especially with a prolonged exposure time.^{4–8} Therefore, accurate and quantitative profiling of air PM composition is of great interest to both environmental and biomedical scientists. Conventional quantitative air PM profiling methods often rely on stationary sites for sampling and sophisticated instruments for analysis.^{9–11} However, it is known

that outdoor air PM levels close to pollutant sources are substantially higher than further away, which may lead to a significant spatial variance between stationary and point-of-origin profiling results.^{12–15} In addition, profiling vertical distribution of air PM constituents is of great importance for assessing pollutants' impact on public health.¹⁶

In recent years, air PM composition profiling using unmanned air vehicles (UAVs) has attained increasing attention as sensor-carrying UAVs permit low-altitude (within 300 m above sea level) air PM composition study at targeted locations, hovering (or maneuvering) in hazardous air space (e.g., over wildfires) or over difficult to access remote areas.^{17,18} Specifically, Chang *et al.* first developed a multicopter-carried whole air sampling system,¹⁹ which was then

used to study the volatile organic compounds (VOCs) in aerial trace gas samples for different types of meteorological conditions;²⁰ Harrison *et al.* used UAVs loaded with commercial sensors to assess the horizontal, vertical, and temporal variability of PM;²¹ UAVs have also been used for volcanic gas sampling²² and greenhouse gases' pollutant measurements.²³ Despite their usefulness in a variety of applications, prompt quantitative analyses of solid-phase or biological air PM constituents using UAVs such as airborne trace metals, viruses, or bacteria are rather scarce due to a lack of accurate, portable quantification techniques. To address this, we recently developed an integrated system consisting of UAV sampling and smartphone-based colorimetric analysis in paper microfluidic devices for accurate quantification of airborne trace metal concentrations.²⁴ Nevertheless, the small weight carrying capacity restricted UAVs' sampling time to be less than 1 h of flight time (typically between 0.5 and 1 h), and according to the US National Ambient Air Quality Standard (NAAQS), reliable analysis of mean spatial distributions of air-quality relevant quantities requires a sampling time range of 1–24 h depending on the pollutant.²⁵ Therefore, the development of a prompt, low-cost, and reliable method for spatiotemporal varying profiling of air PM constituents, particularly in the vertical direction, is still considered as a challenge and is yet to be addressed.

Paper (specifically cellulose paper) has been extensively used in environmental analysis, in particular, air quantity monitoring as it offers particle retention, capillary action triggered self-driven flow, reagents absorbency, cost-effectiveness, biocompatibility, and mechanical merits such as flexibility and lightness. Based on such merits, we aim to address the above issue by presenting a paper-based method for quantitative, reliable profiling of spatiotemporal

variation in air PM compositions [Fig. 1(a)]. The method combines a multirotor UAV with tethered in-flight charging to extend the aerial sampling time to 12–15 flight hours per deployment, thereby effectively improving the sampling reliability issue while maintaining its maneuverability. In addition, the method allows prompt, quantitative analysis of air PM constituents by using smartphone-based colorimetric analysis on paper so that the method is economically efficient and ideally suited to be used in low-resource settings. To the best of our knowledge, this is the first demonstration of a multipoint continuous air PM sampling technique combined with a portable analytical method for constructing a spatiotemporal mapping of air pollutants. We demonstrate the utility of our method by carrying out spatial varying profiling of air PM trace metal constitutes Fe, Mn, and Ni at 4 geographical locations and in the vertical direction at one of the locations in Fuzhou, China, for a period of 21 days, and the results are in agreement with results obtained from using a commercial instrument. Comparing with traditional air balloon monitoring, the tethered UAV method offers precise position control in air, which is essential for close proximity monitoring. Also, it is universally applicable and allows efficient spatiotemporal mapping of air pollutants, by simply redesigning the colorimetric assays.

METHODS AND OPERATING PROCEDURE

System composition

The method is implemented in a system that composes of a self-built air PM sampler, which is reversibly mounted on a foldable multirotor drone (S500, Cangqiong Open Source UAV

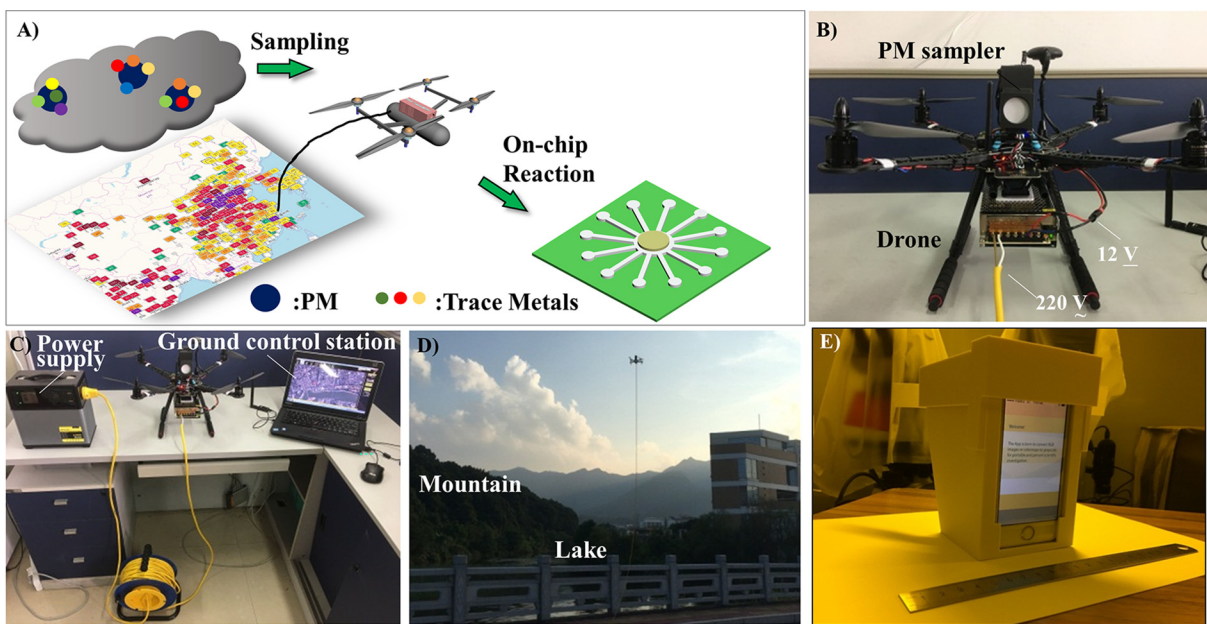


FIG. 1. (a) Schematic of the presented approach; (b) portable PM sampler and voltage transformer mounted on the UAV; (c) the PM sampling system containing power supply, GCS, tether, and UAV; (d) tethered UAV flying above a lake; and (e) iPhone 5s in the black box for image capture.

Inc., Sichuan, China) and tethered to a mobile power supply (S-350, Lueabb, Zhejiang, China) for in-flight sample collection time [Fig. 1(b)]. The collected air PM samples are then processed for downstream composition analysis using a previously reported paper-based microfluidic chip.²⁶ The quantitative profiling of air PM constituents was based on colorimetric principles (Principle in the [supplementary material](#)) and was analyzed remotely using a self-compiled program.

Paper-based device

The detailed device design and the fabrication process flow were reported elsewhere.²⁶ Briefly, a paper chip consisted of one sample inlet ($R = 3.5$ mm), 12 detection reservoirs (DRs) with an optimized radius of 1.5 mm, and 12 internegative control reservoirs (INCs) each with a radius of 2 mm. Hydrophilic channels were designed to connect each of the DRs to the inlet. The devices were made using a batch-to-batch photo-cross-linking, UV exposure technique. As a result, an A4 sized Whatman[®] grade 1 filter paper (Sigma-Aldrich, St. Louis, MO, USA) could produce up to 48 devices in 1 min for a total cost of less than \$10.

Tethered-UAV modification

UAVs that typically run on batteries would have an in-flight time in between 30 and 60 min. To extend it, we design and implement a tethered, continuous energy supply system. The system comprises a ground control station (GCS), a mobile DC-AC inverter ground power station, and a 35 m tether with one end coupling to a UAV carrying voltage transformer that converts station-supplied 220 V AC to a UAV compatible 12 V DC [Fig. 1(c)]. The other end of the tether is coupled to the mobile power station to continuously charge the UAV while hovering. A tension control motor is also coupled to the group power supply, and it receives transmission from sensors mounted within the tether. By adjusting the tension, UAV is allowed to maneuver as commanded by the ground control station. The energy supply system enables continuous UAV hovering at ~ 30 m above the ground for 18–20 h a day depending on environmental conditions [Fig. 1(d)]. However, after 1 day of supplying the power, the mobile power station needs to recharge for 24 h. In addition, the system enables autonomous UAV take-off and landing, thereby only needing one operator for the entire sampling procedure.

Sampler construction

The frame of the PM sampler [Fig. 1(e)] is built by a tabletop 3D printer (Finder[®], FlashForge Inc., Zhejiang, China) and made with lightweight, high tensile strength graphene-enhanced poly lactic acid material (GPLA-5K, PMG 3D Tech, Shanghai, China). A pair of Whatman[®] Grade C filter (Sigma-Aldrich, St. Louis, MO, USA) and a remotely controlled turbofan (San Ace 40, Sanyo Denki, Osaka, Japan) operating on a lithium battery (5 V, 6800 mA, Lede Electronics, Guangdong, China) are included in the sampler assembly. The turbo fan is used to create an air inward flow toward the filter while hovering, and the filters are used to collect air PM samples. The turbo fan is designed to be remotely turned on in order to avoid the collection of any potential contaminants

(e.g., ground dust) as the air is deflected by the action of UAV propellers in motions (i.e., the downwash and upwash effect). The turbo fan is turned on once the UAV has reached its prespecified coordinates and started to hover, when the airflow is relatively stable (preferred for air PM collection). In addition, the air sample inward flow rate can be adjusted by changing the turbofan input voltage.

Sampling efficiency characterization

To maximize the amount of samples collected during the 4–5 h hovering period, first, the sampler is placed in a custom built small “wind tunnel,” which consists of an air blower (CZR, Minfeng Inc., Shanghai, China) and an air flow meter (MF5700, Kongxin Instruments, Nanning, Guangxi, China). The wind tunnel is able to generate a uniform airflow rate ranging from 0 to 17 m/s, and the inward air flow affecting parameters such as the turbo fan drive voltage, sampler angel of elevation, and sampler windward angle are characterized using the setup.

Study sites and sampling conditions

One of the significant advantages of our system is that the portability allows us to freely choose any study sites. A total of 4 sites in Fuzhou city, China, are chosen for our study, each featuring a different geological or sociological significance. Location A is at the foot of a mountain and belongs to a relatively low-population density residential area; location B belongs to a financial district with moderate socioeconomic activities during the day; location C is within an underdeveloped area, but adjacent to a construction site; location D belongs to a residential area with the highest population density and most socioeconomic activities among all sites. Sampling is conducted at each of the above locations 25–30 m above the ground for 4 h per day, and every other day for a total of 21 days, in July 2017. For each sampling day, weather conditions such as temperature, humidity, and natural wind speed of the sites were measured and used as references. In addition, location C is used for vertical profiling of air PM constituents. Samples are collected at the ground level and 10, 20, and 30 m above the ground level for 4 h each, within a day.

Operating procedure

The operation procedure of the method included three steps: in-air PM sampling, colorimetric assay, and data analysis. Starting with PM sampling, the air PM sampler mounting on the tethered UAV was used to collect PM samples at prespecified sampling locations. After the collection period, the sampler was retrieved on the ground, and the collected PM samples (retained on a piece of filter paper) were then digested in an acidic solution followed by neutralizing treatment using a basic solution and pH adjustment using a buffer. For the multiplex quantification of metals Fe, Mn, and Ni, standard solutions of 1,10-phenanthroline, 4-(2-pyridylazo) resorcinol (PAR), and dimethylglyoxime (DMG) were selected as corresponding colorimetric ligands (details presented in the [supplementary material](#)). During the detection process, the colorimetric ligands and the corresponding masking reagents that were used to minimize the effect of interference from other metal ions (Table S1 in the

(supplementary material) were first pipetted onto the designated detection region of the paper chips in sequential orders. Next, the processed metal ion solution was introduced through the inlet of the paper chip. The selected ligands could chelate to metal ions, resulting in distinct coloration associated with different metals. During image capture, the paper chip was inserted into a black box to fix the distance between the device and the smartphone camera as well as shielding the environmental lighting. The black box was made with a carbon fiber reinforced filament (CFPLA, 80SCarbon 2, 80s Studio, Shenzhen, China). A smartphone (iPhone® 5s, Apple Inc., CA, USA) was used to take photos of the device after the assays. The images were then sent to a dedicated server where a program based on an edge-tracking algorithm automatically converted color images to grayscale and determined the corresponding grayscale intensity values in the designated detection areas. The unused sample solutions are stored and sent for analysis using a commercial ICP-OES Analyzer system (Thermo Fisher Scientific, Waltham, MA, USA), and the results were used as a reference. Also, if needed, paper-based analysis can be used to characterize the particle size distribution and the number of particles by using optical microscopy such as scanning electron microscopy (SEM) and transmission electron microscopy (TEM).

RESULTS AND DISCUSSION

Sampler performance characterization

Figures 2(a)–2(c) show the results of sampler air-inflow optimization experiments conducted in the “wind-tunnel.” Of these, Fig. 2(a) demonstrates, at a 20% duty cycle, that the turbo fan RPM showed a linear correlation as a function of the input voltage, and the air inflow rate showed a piece-wise linear correlation instead. Ideally, a higher air-inflow rate was preferred since it enabled more PM to be collected by the filter over unit time. However, an increased rotation speed could affect UAV propellers’ surrounding air flow, decreasing the UAV stability. In addition, the maximum slope of the piecewise linear correlation occurred at 5.5 V. Therefore, an input voltage of 5.5 V was chosen to drive the turbo fan for aerial sampling. Next, the sampler install position onto the UAV including angle of elevation and the windward angel was also optimized in terms of the air-inflow rate. Notably, our UAV was able to maintain stability during flight for an environmental wind speed of less than 17 m/s (Beaufort number 7); therefore, optimization experiments were performed under the environmental wind speed ranging between 0 and 17 m/s. Our experiments indicated in this range, a small elevation angle of 5° generated the best results

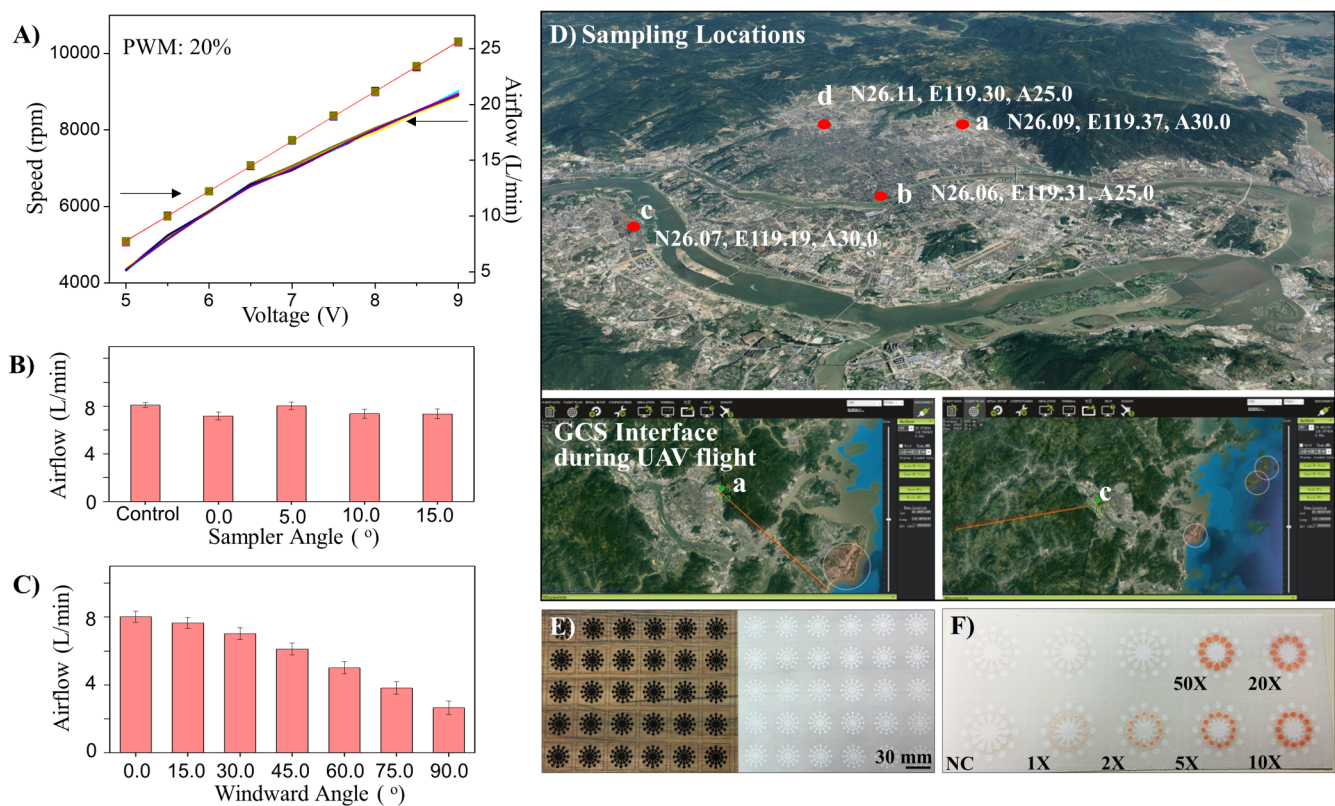


FIG. 2. (a) Rotation speed and air inflow rate vs turbo fan input voltage; (b) effect of the sampler installation angle on air inflow rate; (c) effect of windward angle on air inflow rate; (d) geographic information of the 4 sampling locations; (e) photomask and fabricated paper chips; and (f) representative colorimetric analysis for Fe using the presented method.

[Fig. 2(b)]. In addition, a windward angle of 0° produced the highest air-inflow rate [Fig. 2(c)].

Figure 2(d) visualizes the location and the geological features of the 4 sampling sites in Fuzhou. From the map, all 4 locations were considered as urban areas. However, each site represented a distinct geographical or sociological feature, making them ideal locations for air PM composition spatial variation study. Figure 2(e) shows the fabricated paper chips in an arrayed format, and Fig. 2(f) shows a representative colorimetric analysis for one of the metals tested using our method. A clear color change that was visible to the naked eye was generated to demonstrate different metal concentrations in prepared sample solutions.

Metal assay calibrations

A set of calibration experiments was performed using standard metal salt solutions to correlate gray scale intensities and the metal quantities. As described above, colorimetric ligands per metal ($0.5\ \mu\text{l}$) were added to all 12 DRs and INCs of a device. Masking reagents ($0.5\ \mu\text{l}$) of respective metals were then added to the channels connecting the inlet and the DRs. After drying, standard metal solutions in predetermined concentrations ($6\ \mu\text{l}$) were added to the device inlet and $0.5\ \mu\text{l}$ of deionized water was added to all 12 INCs. For each metal concentration, the average intensity values for all DRs and INCs were obtained from image analysis (excluding the maximum and minimum value), and triplicate measurements

were conducted to verify the validity of our experiment. Using as a background, determined INC values were then subtracted from DRs', and the resulting delta intensity values were plotted against the total metal amount in a DR [Figs. 3(a)–3(c)]. The figures illustrated highly linear correlations between the variables, and the corresponding linear dynamic ranges (LDRs) were then determined to be 170–1440, 9.2–85.2, and 81–684 ng for metals Fe, Mn, and Ni, respectively. The lower limit of the LDRs was then considered as the limit-of-detection (LOD) for the metal assays. In addition, since the total metal amount per cubic meters of air were generally found ranging from nanogram to submicrogram in southern China coastal cities, the LDR of our method was considered appropriate for trace metals quantification.

Specificity study

Masking reagents were used to facilitate any potential interference with other metal ions.^{24,27} Masking is a process in which a substance, without physical separation of it or its reaction products, is so transformed that certain of its reactions are prevented. In our specificity experiment, 8 metals that are commonly found in air PMs (i.e., Hg, Cd, As, Zn, Pb, Ca, Cr, and Cu) were cross-examined. We used specific combinations of chelators to mask the above potential interfering metals in multiplex testing. Specific chelator combinations for Fe, Cu, and Ni are shown in Table S1 in the [supplementary material](#). The experiments started by introducing

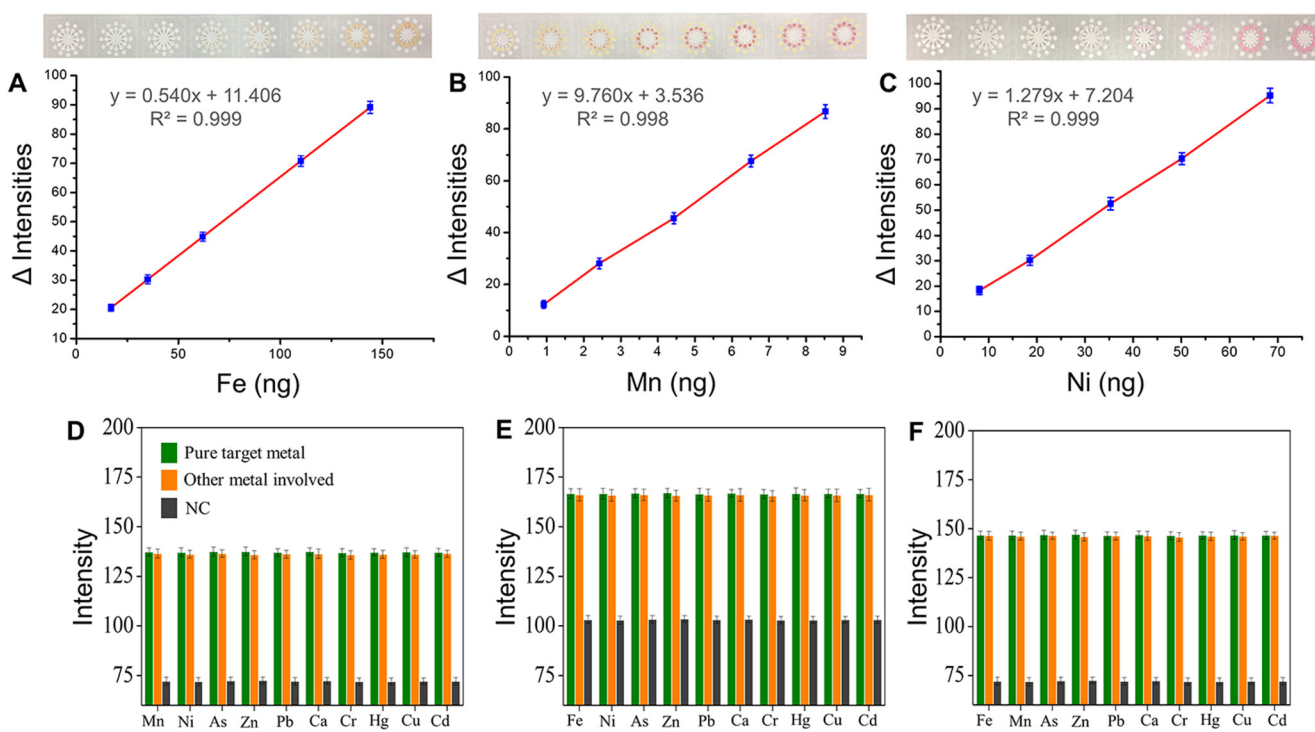


FIG. 3. Metal assays calibration and interference studies. (a)–(c) Images and calibration plots of the colorimetric assays for metals Fe, Mn, and Ni with predetermined concentrations, respectively; (d)–(f) interference studies between Fe, Mn, and Ni with 8 other metals commonly found in air PM.

colorimetric ligands to all 12 DRs on a device. Metal-specific combinations of masking reagents were then added to the device hydrophilic channels. Next, $0.5\text{ }\mu\text{l}$ of target metal solution with a predetermined concentration was added to 1 of the 12 DRs, and $0.5\text{ }\mu\text{l}$ of mixtures between the target metal solution with the same concentration and each of the other 10 metal solutions with a 10-fold concentration increase was then added to 10 of the 11 remaining DRs, while the last DR served as an intranegative control. The resulting image analysis data for Fe, Mn, and Ni are shown in Figs. 3(d)–3(f), respectively. Without subtracting the background, the assay between ligand, target metal and ligand, metal mixtures demonstrated negligible differences in determined intensity values (less than 3%), thus indicating that the potential interfering metal ions did not participate in the assays, thereby confirming the specificity of the method.

Quantitative profiling of air PM composition

Figure 4 uses a color map to illustrate spatial variations in trace metal concentrations, which were determined via both colorimetric assays (SYS) and ICP-OES (ICP), over a 21-day span. Triplicate measurements were made to demonstrate the reproducibility of both analyzing methods (Fig. S4 in the [supplementary material](#)). Notably, the 4 locations were within 5 km radius of the city center, indicating that sampling conditions such as temperature, humidity, and natural wind speed were shared among the locations. Generally, Fuzhou is not a heavy industrial city. Therefore, the determined values of metal amount per unit sample volume (concentration) were expected to be relatively small, and the difference among the locations was minor. However, after examining the data closely, both systematic and spatial dependent differences in quantified metal amount were found, which could be explained by contextual factors such as geological features and

socioeconomic activities. Specifically, for all locations, the quantified metal concentrations were in the order of $\text{Fe} > \text{Ni} > \text{Mn}$. The higher amount of Fe can be explained by being a significant component for crustal soils, whereas both Ni and Mn particles were usually contributed by other anthropogenic sources such as traffic emissions, power-plant operation, and oil-burning.⁹

The data also showed spatially dependent metal amounts. The average metal amounts for 21 days at 4 different locations were 161.88, 14.69, 30.15; 210.10, 25.01, 88.23; 205.08, 17.32, 24.52; and 225.21 29.42, 104.58 ng for Fe, Mn, Ni at locations A–D, respectively. Of these, because location A was a low-population upscale residential area, there were few socioeconomical activities compared to the other sites. The relatively low contribution from anthropogenic sources directly lowers the quantified metal concentrations; the increased socioeconomical activities in location B caused an increase in all quantified Fe, Ni, and Mn concentrations; location C also belonged to a low-population area; therefore, both quantified Ni and Mn concentrations were comparable to location A. However, being close to a construction site significantly increase the Fe concentration when compared with location A. Location D, on the other hand, had the highest average metal concentrations, which was most likely due to contributions from anthropogenic sources. All results determined by our method were in good agreement with the ICP-OES results (within 5% differences).

Our method was also used to characterize the variations in trace metal concentrations in the vertical direction at location C. A sampler was placed on the ground, while an identical sampler was mounted on the UAV for sampling at 10, 20, 30 m above the ground for 4 h, and the corresponding metal amounts were quantified using our method and presented in Fig. 5. Overall, it could be seen that the quantified metal amounts at different heights (ground–30 m) were not significantly different. Specifically, out of the three metals, Fe showed the highest altitude height dependency,

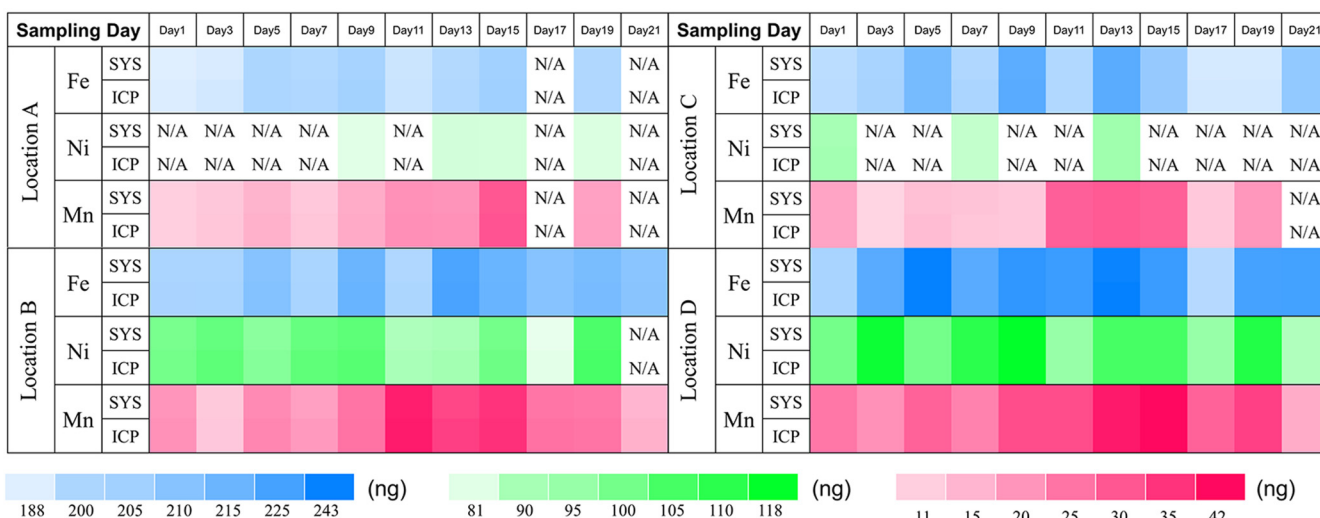


FIG. 4. Spatial variation quantification of representative trace metals Fe, Mn, and Ni in air PM samples from 4 locations over a 21-day (11 sample collection) span.

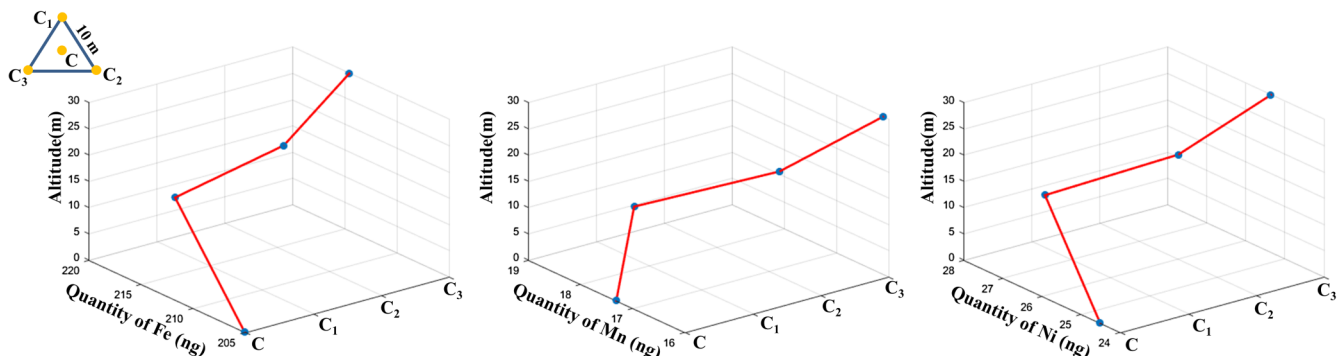


FIG. 5. Vertical profile of Fe, Mn, and Ni concentrations between ground and 30 m above the ground. Aerial sampling locations (C_1 , C_2 , C_3) were within 10 m of the ground sampling location.

as the amount of Fe increased along with height elevation. This potentially could be explained by the construction of high-rise residential buildings at location C. Thus, the utility of using our method for reliable air PM composition spatial variation study was demonstrated.

CONCLUSION

In this study, we developed an integrated method that included tethered aerial sampling, in-flight charging, and quantitative colorimetric analysis in paper microfluidic devices for reliable, economically efficient air PM compositions profiling. Compared with our previous work,²⁶ by significantly increasing sampling time in air and improving assay specificity by using masking reagents, reliable and accurate spatiotemporal quantification of air PM compositions was achieved. Overall, this is the first demonstration of an integrated method that allows the construction of a spatiotemporal mapping of air contaminants in a rapid, portable, and cost-effective manner. We demonstrated the utility of the method by quantitative profiling of airborne trace metals including Fe, Ni, and Mn at 4 geographical locations and in the vertical direction at one of the locations in Fuzhou, China, for a period of 21 days. We found both systematic and spatial dependent differences in a quantified metal amount. Our finding indicated that the variation was mainly caused by human factors, as expected. The quantification results showed good agreements with the results obtained from a commercial ICP-OES instrument, thus signifying the reliability of our method. Notably, although only trace metal quantification is demonstrated in this study, this method is considered as universally applicable and holds great potential to be extended to many fields of environmental research, such as prompt detection of airborne virus, bacteria, or others.

SUPPLEMENTARY MATERIAL

See the [supplementary material](#) for the colorimetric detection principles, the combinations of masking reagents used, the detailed material information, and the complete set of air PM quantification data.

ACKNOWLEDGMENTS

This work was jointly supported by the National Natural Science Foundation of China (NNSFC) under Grant No. 61604042, the Natural Science Foundation of Jiangsu Province under Grant No. SBK2018041725, and the Natural Science Foundation of Fujian Province under Grant No. 2017J01501.

REFERENCES

- M. L. Bell, D. L. Davis, N. Gouveia, V. H. Borja-Aburto, and L. A. Cifuentes, "The avoidable health effects of air pollution in three Latin American cities: Santiago, Sao Paulo, and Mexico City," *Environ. Res.* **100**(3), 431–440 (2006).
- A. Caplin, M. Ghandehari, C. Lim, P. Glimcher, and G. Thurston, "Advancing environmental exposure assessment science to benefit society," *Nat. Commun.* **10**(1), 1236 (2019).
- N. Idros and D. P. Chu, "Triple-indicator-based multidimensional colorimetric sensing platform for heavy metal ion detections," *ACS Sens.* **3**(9), 1756–1764 (2018).
- M. Tomasevic, Z. Vukmirovic, S. Rajsic, M. Tasic, and B. Stevanovic, "Characterization of trace metal particles deposited on some deciduous tree leaves in an urban area," *Chemosphere* **61**(6), 753–760 (2005).
- N. Li, M. Q. Hao, R. F. Phalen, W. C. Hinds, and A. E. Nel, "Particulate air pollutants and asthma—A paradigm for the role of oxidative stress in PM-induced adverse health effects," *Clin. Immunol.* **109**(3), 250–265 (2003).
- J. C. Chow, J. G. Watson, E. M. Fujita, Z. Q. Lu, D. R. Lawson, and L. L. Ashbaugh, "Temporal and spatial variations of PM(2.5) and PM(10) aerosol in the Southern California Air-Quality Study," *Atmos. Environ.* **28**(12), 2061–2080 (1994).
- L. C. Chen and M. Lippmann, "Effects of metals within ambient air particulate matter (PM) on human health," *Inhal. Toxicol.* **21**(1), 1–31 (2009).
- C. Reche *et al.*, "New considerations for PM, black carbon and particle number concentration for air quality monitoring across different European cities," *Atmos. Chem. Phys.* **11**(13), 6207–6227 (2011).
- K. C. Cheng, C. H. Tseng, and L. M. Hildemann, "Using indoor positioning and mobile sensing for spatial exposure and environmental characterizations: Pilot demonstration of PM2.5 mapping," *Environ. Sci. Technol. Lett.* **6**(3), 153–158 (2019).
- Y. J. Zhu, N. Olson, and T. P. Beebe, "Surface chemical characterization of 2.5 μM particulates (PM2.5) from air pollution in Salt Lake City using TOF-SIMS, XPS, and FTIR," *Environ. Sci. Technol.* **35**(15), 3113–3121 (2001).

- ¹¹R. Balasubramanian and W. B. Qian, "Characterization and source identification of airborne trace metals in Singapore," *J. Environ. Monit.* **6**(10), 813–818 (2004).
- ¹²D. J. Wan, L. Song, X. Mao, J. S. Yang, Z. D. Jin, and H. D. Yang, "One-century sediment records of heavy metal pollution on the southeast Mongolian plateau: Implications for air pollution trend in China," *Chemosphere* **220**, 539–545 (2019).
- ¹³P. S. Khillare, S. Balachandran, and B. R. Meena, "Spatial and temporal variation of heavy metals in atmospheric aerosol of Delhi," *Environ. Monit. Assess.* **90**(1–3), 1–21 (2004).
- ¹⁴A. Saffari, N. Daher, M. M. Shafer, J. J. Schauer, and C. Sioutas, "Seasonal and spatial variation of trace elements and metals in quasi-ultrafine (PM 0.25) particles in the Los Angeles metropolitan area and characterization of their sources," *Environ. Pollut.* **181**, 14–23 (2013).
- ¹⁵L. K. Baxter *et al.*, "Influence of human activity patterns, particle composition, and residential Air exchange rates on modeled distributions of PM2.5 exposure compared with central-site monitoring data," *J. Expos. Sci. Environ. Epidemiol.* **23**, 241 (2013).
- ¹⁶H. Zhu *et al.*, "The spatial and vertical distribution of heavy metal contamination in sediments of the three Gorges Reservoir determined by anti-seasonal flow regulation," *Sci. Total Environ.* **664**, 79–88 (2019).
- ¹⁷T. F. Villa, F. Gonzalez, B. Miljievic, Z. D. Ristovski, and L. Morawska, "An overview of small unmanned aerial vehicles for air quality measurements: Present applications and future prospectives," *Sensors* **16**(7), 1072 (2016).
- ¹⁸G. J. Holland, T. McGeer, and H. Youngren, "Autonomous aerosondes for economical atmospheric soundings anywhere on the globe," *Bull. Am. Meteorol. Soc.* **73**(12), 1987–1998 (1992).
- ¹⁹C. C. Chang, J. L. Wang, C. Y. Chang, M. C. Liang, and M. R. Lin, "Development of a multicopter-carried whole air sampling apparatus and its applications in environmental studies," *Chemosphere* **144**, 484–492 (2016).
- ²⁰C. C. Chang *et al.*, "A study of atmospheric mixing of trace gases by aerial sampling with a multi-rotor drone," *Atmos. Environ.* **184**, 254–261 (2018).
- ²¹W. A. Harrison, D. J. Lary, B. J. Nathan, and A. G. Moore, "Using remote control aerial vehicles to study variability of airborne particulates," *Air Soil Water Res.* **8**, 43–51 (2015).
- ²²A. J. S. McGonigle, A. Aiuppa, G. Giudice, G. Tamburello, A. J. Hodson, and S. Gurrieri, "Unmanned aerial vehicle measurements of volcanic carbon dioxide fluxes," *Geophys. Res. Lett.* **35**(6), L06303, <https://doi.org/10.1029/2007GL032508> (2008).
- ²³J. J. Roldan, G. Joosse, D. Sanz, J. del Cerro, and A. Barrientos, "Mini-UAV based sensory system for measuring environmental variables in greenhouses," *Sensors* **15**(2), 3334–3350 (2015).
- ²⁴H. Sun, Y. Jia, H. Dong, and L. X. Fan, "Graphene oxide nanosheets coupled with paper microfluidics for enhanced on-site airborne trace metal detection," *Microsyst. Nanoeng.* **5**, 4 (2019).
- ²⁵EPA (2017), see <https://www.epa.gov/criteria-air-pollutants> for National Ambient Air Quality Standards (NAAQS).
- ²⁶Y. Jia, H. Dong, J. P. Zheng, and H. Sun, "Portable detection of trace metals in airborne particulates and sediments via μPADs and smartphone," *Biomicrofluidics* **11**(6), 064101 (2017).
- ²⁷N. A. Meredith, J. Volckens, and C. S. Henry, "Paper-based microfluidics for experimental design: Screening masking agents for simultaneous determination of Mn(II) and Co(II)," *Anal. Methods* **9**(3), 534–540 (2017).